2023 IEEE/ASME International Conference on Advanced Intelligent Mechatronics (AIM)
June 28-30, 2023. Seattle, Washington, USA

Admittance-Based Non-Singular Terminal Sliding Mode Control of Multiple Cooperative Manipulators

Lucas Wan, *Student Member, IEEE*, Ya-Jun Pan, *Senior Member, IEEE*,
and Qiguang Chen, *Student Member, IEEE*

***Abstract*— This paper introduces a novel decentralized control framework that integrates admittance control, non-singular terminal sliding mode (NTSM) control, and load distribution to cooperatively manipulate a single object with multiple robotic manipulators. Admittance control grants the system a level of compliance for safe human-robot physical interaction. The admittance controller maintains all communication between the manipulators. The NTSM controller provides accurate tracking of the manipulators in the presence of disturbances and dynamic model uncertainties. A decentralized load distribution method is designed to minimize the internal forces on the object. The proposed framework is applied to numerical simulations of a team of three 3-DOF robotic manipulators to demonstrate its effectiveness in cooperative manipulation tasks.**

I. Introduction

Collaborative and cooperative robotic manipulators are designed to work alongside humans in a shared workspace. These robots are becoming increasingly popular in a variety of industries, including manufacturing, healthcare, and construction. Introducing compliance into the control structure allows humans to physically interact with the robots, improving productivity for collaborative tasks. Multiple manipulators can work together cooperatively to lift and move heavy or odd-shaped objects or coordinate to assemble a product. This paper introduces a novel decentralized control framework that combines compliant admittance control, nonlinear non-singular terminal sliding mode (NTSM) control, and load distribution to cooperatively manipulate a single object.

Admittance and impedance control are beneficial for human-robot interaction, as they allow a manipulator to respond to physical interactions in a safe, compliant, and intuitive manner. In [1], an admittance velocity controller is combined with a human intention estimator and load distribution for a collaborative dual-arm task. In [2], an admittance controller is combined with a neural network controller for a centralized multi-manipulator system following a desired object trajectory. In [3], a decentralized impedance controller is applied to a dual-arm system with the goal of limiting the internal and contact forces of the object. In [4], a passivity-based leader-follower admittance controller is applied to a dual-arm system.

A NTSM controller enables a robot to exhibit robust, stable, and accurate behaviour in various operating conditions, including disturbances and model uncertainties. Compared to traditional sliding mode control (SMC), NTSM control is able to converge faster in a finite time and avoid the singularity issue [5]. In [6], a multi-manipulator teleoperation system with adaptive NTSM control is designed to provide the environmental wrench feedback. In [7], a distributed sliding mode controller is applied for the coordinated tracking of multiple Euler-Lagrange systems.

Work has been done in combining the admittance control with NTSM control for a single manipulator in the literature. In [8], a fractional-order sliding mode controller is combined with admittance control for a single agent telerobotic system. In [9], PID control, SMC, and admittance control are implemented into a controller and applied to a single manipulator. In [10], a non-singular fixed-time sliding mode controller is combined with an admittance controller and applied to a manipulator. To the author's knowledge, admittance and NTSM control has not been applied to multiple manipulators in previous literature.

When multiple manipulators are grasping a single object, it is important to distribute the load appropriately among the manipulators to avoid the risk of overloading a single manipulator. Additionally, a suitable load distribution is necessary to minimize the internal wrench acting on the the object, which improves the precision of the system and protects the object from being damaged. In [11], a strategy is proposed for a heterogeneous load distribution and in [12], a strategy is proposed for the dynamic load allocation for multi-robot manipulation tasks.

The design of a decentralized system involving multiple manipulators offers several benefits over a centralized system. In a decentralized setup, where each manipulator operates independently based on its local information, the system demonstrates superior flexibility in response to changes in the topology. Decentralized systems are also more robust and reliable as they eliminate single points of failure. These advantages are particularly beneficial in applications such as search and rescue operations involving teams of mobile manipulators, as well as modular manufacturing lines.

This work is motivated by the need for a cooperative

This work was supported in part by funding from the Natural Sciences and Engineering Council (NSERC) and the Government of Nova Scotia, Canada.

Lucas Wan, Ya-Jun Pan, and Qiguang Chen are with the Department of Mechanical Engineering, Dalhousie University, Halifax, Canada, B3H 4R2. (e-mails: lucas.wan@dal.ca, yajun.pan@dal.ca, qg234631@dal.ca).

multi-manipulator framework that is flexible, suited for physical human-robot interaction, and robust against significant internal disturbances and model uncertainties. A decentralized formulation of the load distribution is presented. The state communication between manipulators is confined to the admittance controller to minimize the complexity of the nonlinear NTSM controller. Simulations are conducted for three 3-degree of freedom (DOF) manipulators grasping a single object and the proposed framework is compared to an impedance controller to demonstrate the advantages in tracking accuracy and response to external wrenches.

II. Preliminaries

A. Graph Theory

A directed graph depicts the communication structure of a networked multi-robot system. A directed graph is denoted by $\mathcal{G} = \{\mathcal{V}, \mathcal{E}, \mathcal{A}\}$. The agents are denoted by $\mathcal{V} = \{1, 2, \ldots, N\}$ and the communication channels are denoted by $\mathcal{E} \subseteq \mathcal{V} \times \mathcal{V}$. A directed edge, $(i, j) \in \mathcal{E}$, indicates that agent j is receiving information from agent i. The adjacency matrix $\mathcal{A} = [a_{ij}]_{n\times n} \in R^{n\times n}$ denotes the communication between the follower agents, where $a_{ij} = 1$ for $(j, i) \in \mathcal{E}$, otherwise $a_{ij} = 0$. The communication between the leader and followers can be denoted by $\mathcal{B} = [b_1\ b_2\ \ldots\ b_m]^T$, where $b_i = 1$ if the i^{th} follower is connected to the leader, otherwise $b_i = 0$. In this paper, the desired state of the object represents the virtual leader.

B. Robot Manipulator Dynamics

Consider a group of n-DOF robot manipulators with the joint space dynamics of the form

$$\mathcal{M}_i(\boldsymbol{q}_i)\ddot{\boldsymbol{q}}_i + \mathcal{C}_i(\boldsymbol{q}_i, \dot{\boldsymbol{q}}_i)\dot{\boldsymbol{q}}_i + \mathcal{G}_i(\boldsymbol{q}_i) = \boldsymbol{\tau}_i + \boldsymbol{\tau}_{e_i} + \boldsymbol{\tau}_{fd_i}, \quad (1)$$

where $i = \{1, 2, \ldots, N\}$, N is the number of manipulators, $\boldsymbol{q}_i, \dot{\boldsymbol{q}}_i, \ddot{\boldsymbol{q}}_i \in \mathbb{R}^n$ are the joint position, velocity, and acceleration vectors, respectively, $\mathcal{M}_i(\boldsymbol{q}_i) \in \mathbb{R}^{n\times n}$ is the inertia matrix, $\mathcal{C}_i(\boldsymbol{q}_i, \dot{\boldsymbol{q}}_i) \in \mathbb{R}^{n\times n}$ is the Coriolis and centripetal torque matrix, $\mathcal{G}_i(\boldsymbol{q}_i) \in \mathbb{R}^n$ is the gravitational torque vector, $\boldsymbol{\tau}_i \in \mathbb{R}^n$ is the control input torque vector, $\boldsymbol{\tau}_{e_i} \in \mathbb{R}^n$ is the external torque exerted on the manipulator, $\boldsymbol{\tau}_{fd_i} = \boldsymbol{\tau}_{f_i} + \boldsymbol{\tau}_{d_i} \in \mathbb{R}^n$ is the summation of the internal torque friction, $\boldsymbol{\tau}_{f_i}$, and unmodelled dynamics, $\boldsymbol{\tau}_{d_i}$, due to modelling inaccuracies or external disturbances, and n is the number of joints. To facilitate the motion of the manipulated object, the dynamics of the robot manipulators may be represented in a 6-dimensional Cartesian space as

$$\bar{\mathcal{M}}_i(\boldsymbol{q}_i)\ddot{\boldsymbol{x}}_i + \bar{\mathcal{C}}_i(\boldsymbol{q}_i, \dot{\boldsymbol{q}}_i)\dot{\boldsymbol{x}}_i + \bar{\mathcal{G}}_i(\boldsymbol{q}_i) = \boldsymbol{u}_i + \boldsymbol{h}_{e_i} + \boldsymbol{h}_{fd_i}. \quad (2)$$

The end-effector pose is denoted as $\boldsymbol{x}_i = \begin{bmatrix}\boldsymbol{p}_i^T & \boldsymbol{\xi}_i^T\end{bmatrix}^T \in \mathbb{R}^7$ where $\boldsymbol{p}_i \in \mathbb{R}^3$ is the translational position and $\boldsymbol{\xi}_i = \begin{bmatrix}\eta_i & \boldsymbol{\epsilon}_i^T\end{bmatrix}^T \in \mathrm{S}^3 \subset \mathbb{R}^4$ is the orientation in the form of a unit quaternion. The quaternion is made up of η_i, a scalar denoting the real part, and $\boldsymbol{\epsilon}_i = \begin{bmatrix}\epsilon_{i_1} & \epsilon_{i_2} & \epsilon_{i_3}\end{bmatrix}^T$, a vector denoting the imaginary part. The end-effector velocity and acceleration are denoted as $\dot{\boldsymbol{x}}_i = \begin{bmatrix}\dot{\boldsymbol{p}}_i^T & \boldsymbol{\omega}_i^T\end{bmatrix}^T \in \mathbb{R}^6, \ddot{\boldsymbol{x}}_i = \begin{bmatrix}\ddot{\boldsymbol{p}}_i^T & \dot{\boldsymbol{\omega}}_i^T\end{bmatrix}^T \in \mathbb{R}^6$, where $\boldsymbol{\omega}_i,\ \dot{\boldsymbol{\omega}}_i \in \mathbb{R}^3$ are the angular velocity and acceleration of the end-effector, respectively. The angular velocity and acceleration may be calculated from the orientation quaternion by $\boldsymbol{\omega}_i = 2E_i(\boldsymbol{\xi})^T\dot{\boldsymbol{\xi}}_i$ and $\dot{\boldsymbol{\omega}}_i = 2E_i(\boldsymbol{\xi})^T\ddot{\boldsymbol{\xi}}_i$, where $E_i(\boldsymbol{\xi}) = \begin{bmatrix}-\boldsymbol{\epsilon}_i & (\eta_i I_3 - S(\boldsymbol{\epsilon}_i))^T\end{bmatrix}^T \in \mathbb{R}^{4\times 3}$ and $S(*)$ is the skew-symmetric matrix operator [13]. The full state is denoted as $\boldsymbol{X}_i = \{\boldsymbol{x}_i,\ \dot{\boldsymbol{x}}_i,\ \ddot{\boldsymbol{x}}_i\}$.

The end-effector velocity and joint velocity are related by the Jacobian matrix, $J_i(\boldsymbol{q}_i) = \begin{bmatrix}J_{p_i}^T(\boldsymbol{q}_i) & J_{\omega_i}^T(\boldsymbol{q}_i)\end{bmatrix}^T \in \mathbb{R}^{6\times n}$, where $J_{p_i}(\boldsymbol{q}_i) \in \mathbb{R}^{3\times n}$ is the translational Jacobian matrix and $J_{\omega_i}(\boldsymbol{q}_i) \in \mathbb{R}^{3\times n}$ is the angular Jacobian matrix, through $\dot{\boldsymbol{x}}_i = J_{p_i}(\boldsymbol{q}_i)\dot{\boldsymbol{q}}_i$ and $\boldsymbol{\omega}_i = J_{\omega_i}(\boldsymbol{q}_i)\dot{\boldsymbol{q}}_i$.

The wrench variables are denoted as $\boldsymbol{h}_{*_i} = \begin{bmatrix}\boldsymbol{F}_{*_i}^T & \boldsymbol{\tau}_{*_i}^T\end{bmatrix}^T$, where $\boldsymbol{F}_{*_i}$ and $\boldsymbol{\tau}_{*_i}$ denote the force and torque, respectively, and are related to the joint space variables where $\boldsymbol{u}_i = J_i(\boldsymbol{q}_i)\boldsymbol{\tau}_i \in \mathbb{R}^6$ is the force control input, $\boldsymbol{h}_{e_i} = J_i(\boldsymbol{q}_i)\boldsymbol{\tau}_{e_i} \in \mathbb{R}^6$ is the external wrench exerted on the manipulator's end-effector, and $\boldsymbol{h}_{fd_i} = J_i(\boldsymbol{q}_i)\boldsymbol{\tau}_{fd_i} \in \mathbb{R}^6$ is the internal wrench due to friction and unmodelled dynamics.

Property 1: The Cartesian parametric matrices in (2) are related to the joint space parametric matrices in (1) by

$$\begin{aligned}\bar{\mathcal{M}}_i(\boldsymbol{q}_i) &= J_i(\boldsymbol{q}_i)^{-T}\mathcal{M}_i(\boldsymbol{q}_i)J_i(\boldsymbol{q}_i)^{-1},\\ \bar{\mathcal{C}}_i(\boldsymbol{q}_i, \dot{\boldsymbol{q}}_i) &= J_i(\boldsymbol{q}_i)^{-T}(\mathcal{C}_i(\boldsymbol{q}_i, \dot{\boldsymbol{q}}_i)\\ &\quad - \mathcal{M}_i(\boldsymbol{q}_i)J_i(\boldsymbol{q}_i)^{-1}\dot{J}_i(\boldsymbol{q}_i))J_i(\boldsymbol{q}_i)^{-1},\\ \bar{\mathcal{G}}_i(\boldsymbol{q}_i) &= J_i(\boldsymbol{q}_i)^{-T}\mathcal{G}_i(\boldsymbol{q}_i).\end{aligned}$$

Property 2: The inertia matrix, $\bar{\mathcal{M}}_i(\boldsymbol{q}_i)$, is symmetric positive-definite and $\dot{\bar{\mathcal{M}}}_i(\boldsymbol{q}_i) - 2\bar{\mathcal{C}}_i(\boldsymbol{q}_i, \dot{\boldsymbol{q}}_i)$ is skew-symmetric.

C. Object Dynamics

The dynamics of the object can be expressed as

$$\mathcal{M}_o\ddot{\boldsymbol{x}}_o + \mathcal{C}_o\dot{\boldsymbol{x}}_o + \mathcal{G}_o = \boldsymbol{h}_o + \boldsymbol{h}_e, \quad (3)$$

where

$$\mathcal{M}_o = \begin{bmatrix}m_o I_3 & 0_3\\ 0_3 & I_o\end{bmatrix}, \mathcal{C}_o = \begin{bmatrix}0_3 & 0_3\\ 0_3 & \omega_o I_o\end{bmatrix}, \mathcal{G}_o = \begin{bmatrix}-m_o g\\ \boldsymbol{0}_{3\times 1}\end{bmatrix},$$

and m_o is the object's mass, $I_o \in \mathbb{R}^{3\times 3}$ is the object's inertia, ω_o is the angular velocity of the object, and g is the gravitational acceleration constant.

Assumption 1: The manipulated object is rigid and the end-effectors of each manipulator are assumed to be rigidly connected to the object.

D. State Constraints

Assumption 1 implies that the position of each manipulator end-effector remains constant relative to the object's coordinate frame. Therefore, the following constraints [11], define the desired state of each manipulator, $\boldsymbol{X}_{d_i}$, based on the state of the object $\boldsymbol{X}_o$:

$$\begin{aligned}\boldsymbol{p}_{d_i} &= \boldsymbol{p}_o + R_o\boldsymbol{r}_i,\\ \dot{\boldsymbol{p}}_{d_i} &= \dot{\boldsymbol{p}}_o + \boldsymbol{\omega}_o \times \boldsymbol{r}_i,\\ \ddot{\boldsymbol{p}}_{d_i} &= \ddot{\boldsymbol{p}}_o + \dot{\boldsymbol{\omega}}_o \times \boldsymbol{r}_i + \boldsymbol{\omega}_o \times (\boldsymbol{\omega}_o \times \boldsymbol{r}_i),\\ \boldsymbol{\xi}_{d_i} &= \boldsymbol{\xi}_o * \boldsymbol{\delta}_{\xi_i},\ \boldsymbol{\omega}_{d_i} = \boldsymbol{\omega}_o,\ \dot{\boldsymbol{\omega}}_{d_i} = \dot{\boldsymbol{\omega}}_o,\end{aligned}$$

where $R_o \in \mathrm{SO}(3) \subset \mathbb{R}^9$ is the rotation matrix converted from the object orientation unit quaternion, $\boldsymbol{r}_i \in \mathbb{R}^3$ is the displacement between the object center of mass and the i^{th} manipulator's grasping point, $\boldsymbol{\delta}_{\xi_i} \in \mathrm{S}^3 \subset \mathbb{R}^4$ is the relative orientation between the object and the i^{th} manipulator, and $*$ represents quaternion multiplication. Due to the kinematic constraints implied by Assumption 1, $\boldsymbol{r}_i$ and $\boldsymbol{\delta}_{\xi_i}$ are constants.

E. Load Distribution

To minimize the internal wrenches applied to the object, consider that $\boldsymbol{h}_o$ in Eq. (3) is the desired object wrench. The wrench allocated to each manipulator can be calculated as

$$\begin{bmatrix} \boldsymbol{h}_{d_i} \\ \vdots \\ \boldsymbol{h}_{d_N} \end{bmatrix} = G^{\dagger} \boldsymbol{h}_o, \tag{4}$$

where $G^{\dagger}$ is the Moore-Penrose inverse of the grasping matrix,

$$G = \begin{bmatrix} I_3 & 0_3 & \cdots & I_3 & 0_3 \\ S(\boldsymbol{r}_1) & I_3 & \cdots & S(\boldsymbol{r}_N) & I_3 \end{bmatrix}.$$

F. Frame Transformations

For the different manipulator states to be used in the decentralized controllers, they must be in the correct coordinate frame. To convert between the world frame, ${}^{w}\Sigma$, and each manipulator's frame, ${}^{i}\Sigma$, the transformation ${}^{w}T^{i} = \{{}^{w}R^{i}, {}^{w}R^{i}_{q}, {}^{w}\boldsymbol{\Delta}^{i}\}$ is applied as

$$\begin{aligned} &{}^{i}\boldsymbol{x} = {}^{w}R^{i}({}^{w}\boldsymbol{x} - {}^{w}\boldsymbol{\Delta}^{i}),\ {}^{i}\dot{\boldsymbol{x}} = {}^{w}R^{i} \cdot {}^{w}\dot{\boldsymbol{x}},\ {}^{i}\ddot{\boldsymbol{x}} = {}^{w}R^{i} \cdot {}^{w}\ddot{\boldsymbol{x}}, \\ &{}^{i}\boldsymbol{\xi} = {}^{w}R^{i}_{q} \cdot {}^{w}\boldsymbol{\xi},\ {}^{i}\boldsymbol{\omega} = {}^{w}R^{i} \cdot {}^{w}\boldsymbol{\omega},\ {}^{i}\dot{\boldsymbol{\omega}} = {}^{w}R^{i} \cdot {}^{w}\dot{\boldsymbol{\omega}}, \end{aligned}$$

where ${}^{w}\boldsymbol{\Delta}^{i} \in \mathbb{R}^3$ is the relative translation between the world frame and the i-th frame, ${}^{w}R^{i} = {}^{w}R^{i}_{z}\,{}^{w}R^{i}_{y}\,{}^{w}R^{i}_{x} \in \mathbb{R}^{3\times3}$ is the relative rotation between the world frame and the i-th frame about the x, y, and z axes, and ${}^{w}R^{i}_{q} = {}^{w}R^{i}_{q_z}\,{}^{w}R^{i}_{q_y}\,{}^{w}R^{i}_{q_x} \in \mathrm{S}^3 \subset \mathbb{R}^4$ is the relative quaternion rotation.

G. Decentralized State Constraints

In cases where every manipulator does not receive the desired object state, each agent may use the reference state of their neighbours, $\boldsymbol{X}_{r_j}$, in the controller. Note that $\tilde{(*)}^{j}$ represents the estimated value of $(*)$ based on the information from Agent j. First, the orientation of the object is estimated as

$$\tilde{\boldsymbol{\xi}}^{j}_{o} = \boldsymbol{\xi}_{r_j} * \boldsymbol{\delta}^{-1}_{\xi_j},\ \tilde{\boldsymbol{\omega}}^{j}_{o} = \boldsymbol{\omega}_{r_j},\ \tilde{\dot{\boldsymbol{\omega}}}^{j}_{o} = \dot{\boldsymbol{\omega}}_{r_j}.$$

Then, the rotation matrix, $\tilde{R}^{j}_{o}$ can be converted from $\tilde{\boldsymbol{\xi}}^{j}_{o}$ and the full reference state of the i-th agent based on the j-th agent's information, $\tilde{\boldsymbol{X}}^{j}_{r_i}$, can be estimated as

$$\begin{aligned} \tilde{\boldsymbol{p}}^{j}_{r_i} &= \boldsymbol{p}_{r_j} + \tilde{R}^{j}_{o}(\boldsymbol{r}_i - \boldsymbol{r}_j), \\ \tilde{\dot{\boldsymbol{p}}}^{j}_{r_i} &= \dot{\boldsymbol{p}}_{r_j} + \tilde{\boldsymbol{\omega}}^{j}_{o} \times (\boldsymbol{r}_i - \boldsymbol{r}_j), \\ \tilde{\ddot{\boldsymbol{p}}}^{j}_{r_i} &= \ddot{\boldsymbol{p}}_{r_j} + \tilde{\dot{\boldsymbol{\omega}}}^{j}_{o} \times (\boldsymbol{r}_i - \boldsymbol{r}_j) + \tilde{\boldsymbol{\omega}}^{j}_{o} \times (\tilde{\boldsymbol{\omega}}^{j}_{o} \times (\boldsymbol{r}_i - \boldsymbol{r}_j)), \\ \tilde{\boldsymbol{\xi}}^{j}_{r_i} &= \tilde{\boldsymbol{\xi}}^{j}_{o} * \boldsymbol{\delta}_{\xi_i},\ \tilde{\boldsymbol{\omega}}^{j}_{r_i} = \tilde{\boldsymbol{\omega}}^{j}_{o},\ \tilde{\dot{\boldsymbol{\omega}}}^{j}_{r_i} = \tilde{\dot{\boldsymbol{\omega}}}^{j}_{o}. \end{aligned}$$

H. Decentralized Load Distribution

Similarly, each agent may use the measured state of their neighbours, $\boldsymbol{X}_j$, to calculate the object dynamics and the load distribution. First the object state is estimated as

$$\begin{aligned} \tilde{\boldsymbol{\omega}}^{j}_{o} &= \boldsymbol{\omega}_j,\ \tilde{\dot{\boldsymbol{\omega}}}^{j}_{o} = \dot{\boldsymbol{\omega}}_j, \\ \tilde{\boldsymbol{p}}^{j}_{o} &= \dot{\boldsymbol{p}}_j - \tilde{\boldsymbol{\omega}}^{j}_{o} \times \boldsymbol{r}_j, \\ \tilde{\ddot{\boldsymbol{p}}}^{j}_{o} &= \ddot{\boldsymbol{p}}_j - \tilde{\dot{\boldsymbol{\omega}}}^{j}_{o} \times \boldsymbol{r}_j - \tilde{\boldsymbol{\omega}}^{j}_{o} \times (\tilde{\boldsymbol{\omega}}^{j}_{o} \times \boldsymbol{r}_j). \end{aligned}$$

Then, the estimate states are used in Eqs. (3) and (4) to calculate $\tilde{\boldsymbol{h}}^{j}_{d_i}$.

III. Controller Design

The control framework is shown in Fig. 1. Each state is transformed to the appropriate frame before it is input to a controller. The dashed lines denote optional communication channels based on the communication network.

A. Admittance Controller

The admittance controller is designed to track the desired state of the object and grant safe, compliant reactions to external wrenches applied by the environment or humans. The admittance model is designed as

$$M_{d_i}\ddot{\boldsymbol{e}}_{a_i} + D_{d_i}\dot{\boldsymbol{e}}_{a_i} + K_{d_i}\boldsymbol{e}_{a_i} = b_i\boldsymbol{h}_{e_i}, \tag{5}$$

where $M_{d_i}, D_{d_i}, K_{d_i} \in \mathbb{R}^{6\times6}$ are positive-definite diagonal gain matrices that represent the desired inertia, damping, and stiffness, respectively. Tuning these parameters influences the manipulators' response to external wrenches. The error terms are designed as

$$\begin{aligned} \boldsymbol{e}_{a_i} &= \sum_{j=1}^{N} a_{ij} \begin{bmatrix} \boldsymbol{p}_{r_i} - \boldsymbol{p}^{j}_{r_i} \\ \mathbb{E}(\boldsymbol{\xi}_{r_i}, \boldsymbol{\xi}^{j}_{r_i}) \end{bmatrix} + b_i \begin{bmatrix} \boldsymbol{p}_{r_i} - \boldsymbol{p}_{d_i} \\ \mathbb{E}(\boldsymbol{\xi}_{r_i}, \boldsymbol{\xi}_{d_i}) \end{bmatrix}, \\ \dot{\boldsymbol{e}}_{a_i} &= \sum_{j=1}^{N} a_{ij}(\dot{\boldsymbol{x}}_{r_i} - \dot{\boldsymbol{x}}^{j}_{r_i}) + b_i(\dot{\boldsymbol{x}}_{r_i} - \dot{\boldsymbol{x}}_{d_i}), \\ \ddot{\boldsymbol{e}}_{a_i} &= \sum_{j=1}^{N} a_{ij}(\ddot{\boldsymbol{x}}_{r_i} - \ddot{\boldsymbol{x}}^{j}_{r_i}) + b_i(\ddot{\boldsymbol{x}}_{r_i} - \ddot{\boldsymbol{x}}_{d_i}), \end{aligned}$$

where $\mathbb{E}(\boldsymbol{\xi}_1, \boldsymbol{\xi}_2) = (\eta_1\eta_2 + \boldsymbol{\epsilon}_1^T\boldsymbol{\epsilon}_2)(-\eta_1\boldsymbol{\epsilon_2} + \eta_2\boldsymbol{\epsilon_1} - S(\boldsymbol{\epsilon_1})\boldsymbol{\epsilon_2}) \in \mathbb{R}^3$. To generate the compliant behaviour, Eq. (5) can be arranged into

$$\begin{aligned} \ddot{\boldsymbol{x}}_{r_i} = \bar{N}_i^{-1}\Big(&M_{d_i}^{-1}(b_i\boldsymbol{h}^{e}_{i} - D_{d_i}\dot{\boldsymbol{e}}_{a_i} - K_{d_i}\boldsymbol{e}_{a_i}) \\ &+ \sum_{j=1}^{N} a_{ij}\ddot{\boldsymbol{x}}_{r_j} + b_i\ddot{\boldsymbol{x}}_{d_i}\Big), \end{aligned} \tag{6}$$

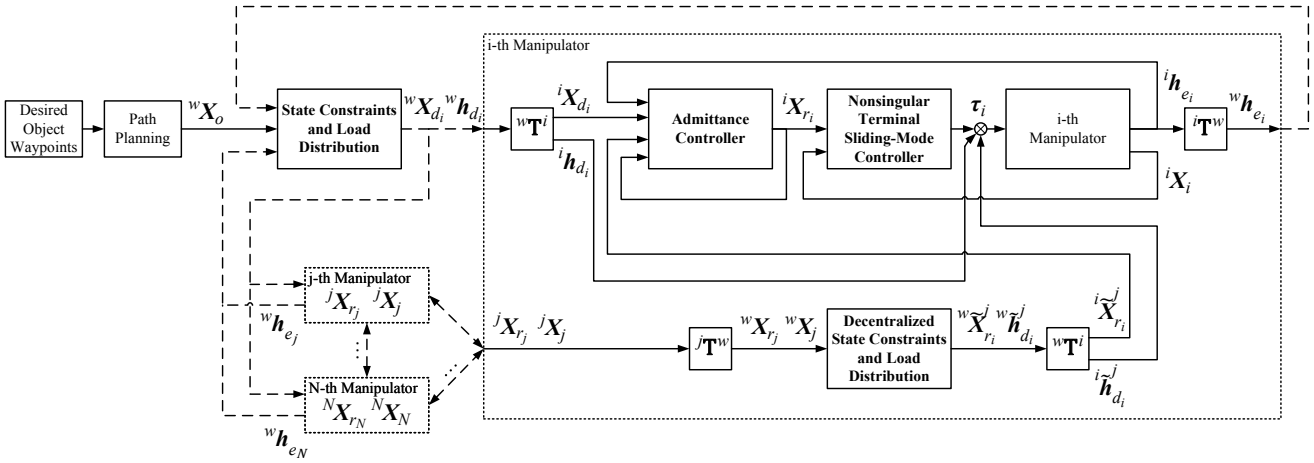

Fig. 1. Schematic diagram of the proposed approach

where $\bar{N}_i = \sum_{j=1}^{N} a_{ij} + b_i$. The reference state, $\boldsymbol{X}_{r_j}$, is used instead of the measured state, $\boldsymbol{X}_j$, because the measured state is influenced by friction and unmodelled dynamics which may cause inaccuracies in the admittance controller. The $b_i \boldsymbol{h}_i^e$ term is implemented so that only the agents connected to the leader consider the external wrench because the admittance controller indirectly considers the external wrench through the communicated reference states.

Assumption 2: The agents connected to the leader do not receive information from other agents and the external wrench on their end-effectors, $\boldsymbol{h}_{e_i}$, is measurable.

B. Non-singular Terminal Sliding Mode Control

The NTSM controller is designed to accurately track the reference state output from the admittance controller while remaining robust to internal friction and unmodelled dynamics. There is no communication in the error terms of the NTSM controller. The sliding surface is expressed as

$$\boldsymbol{s}_i = \boldsymbol{e}_i + \beta_i \dot{\boldsymbol{e}}_i^{\alpha_i}, \tag{7}$$

where $\beta_i > 0$, $\alpha_i = p_i/q_i$, $p_i > 0$ and $q_i > 0$ are adjacent odd numbers such that $1 < \alpha_i < 2$, and

$$\boldsymbol{e}_i = \begin{bmatrix} \boldsymbol{p}_i - \boldsymbol{p}_{r_i} \\ \mathbb{E}(\boldsymbol{\xi}_i, \boldsymbol{\xi}_{r_i}) \end{bmatrix},$$
$$\dot{\boldsymbol{e}}_i = \dot{\boldsymbol{x}}_i - \dot{\boldsymbol{x}}_{r_i}.$$

The controller is designed as

$$\boldsymbol{u}_i = \bar{\mathcal{C}}_i(\boldsymbol{q}_i, \dot{\boldsymbol{q}}_i)\dot{\boldsymbol{x}}_i + \bar{\mathcal{G}}_i(\boldsymbol{q}_i) + \bar{\mathcal{M}}_i(\boldsymbol{q}_i)\Big(\frac{-\dot{\boldsymbol{e}}_i^{2-\alpha_i}}{\alpha_i \beta_i}$$
$$+ \ddot{\boldsymbol{x}}_{r_i} - \kappa_i \tanh(k_{s_i}\boldsymbol{s}_i)\Big) + \bar{N}_i^{-1}\Big(\sum_{j=1}^{N} a_{ij}\tilde{\boldsymbol{h}}_{d_i}^{j} + b_i \boldsymbol{h}_{d_i}\Big), \tag{8}$$

where $\kappa_i > 0$ is the positive control gain, and $k_{s_i} > 0$ is a design parameter that gives a trade-off between reducing chattering and tracking performance. The control input is applied in joint space, where $\boldsymbol{\tau}_i = J_i(\boldsymbol{q}_i)^T \boldsymbol{u}_i$. Note that the stability proof is omitted here due to limited space.

IV. Simulation Studies

In this section, the proposed framework is validated with numerical simulations of three homogeneous 3-DOF manipulators moving an object. First, the admittance-based NTSM control framework is compared to the impedance control to demonstrate the advantages of the proposed controller. Then, a decentralized case with time-varying communication delays is presented to validate the distributed components of the framework. Due to the limited DOFs of the manipulators, only translational motion is considered and the orientation of the object remains constant. It is assumed that the end-effectors may rotate freely about the grasp points of the object. The set-up of three manipulators is shown in Fig. 2.

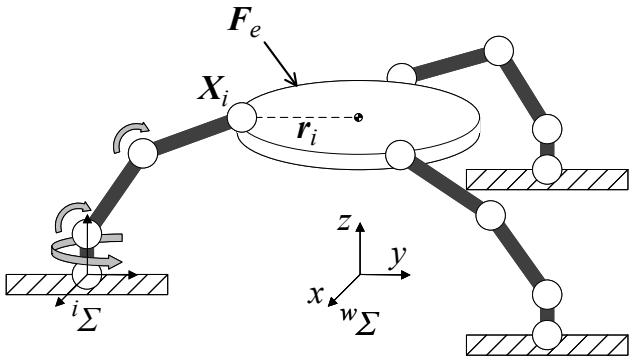

Fig. 2. Multi-manipulator set-up

A. Robot Manipulator Model

The manipulators are modelled as Phantom Omni haptic devices. The dynamic model parameters used to build Eq. (1) are described in [14]. The manipulator's dynamics are simulated with $0.8\mathcal{M}_i$, $0.8\mathcal{C}_i$, and $0.8\mathcal{G}_i$ to provide model

uncertainty. The internal frictions are modelled as a combined viscous friction, $\boldsymbol{\tau}_{fv_i}$, and Coulomb friction, $\boldsymbol{\tau}_{fc_i}$:

$$\boldsymbol{\tau}_{f_i} = \boldsymbol{\tau}_{fv_i}(\dot{\boldsymbol{q}}_i) + \boldsymbol{\tau}_{fc_i}(\dot{\boldsymbol{q}}_i),$$
$$\boldsymbol{\tau}_{fv_i} = \begin{bmatrix}0.002\dot{\boldsymbol{q}}_{1_i}, & 0.01\dot{\boldsymbol{q}}_{2_i}, & 0.01\dot{\boldsymbol{q}}_{3_i}\end{bmatrix}^T,$$
$$\boldsymbol{\tau}_{fc_i} = \begin{bmatrix}0.02\text{sgn}(\dot{\boldsymbol{q}}_{1_i}), & 0.02\text{sgn}(\dot{\boldsymbol{q}}_{2_i}), & 0.002\text{sgn}(\dot{\boldsymbol{q}}_{3_i})\end{bmatrix}^T.$$

The control input torque is saturated with absolute torque limits of $|\boldsymbol{\tau}|_{max} = \begin{bmatrix}0.30, & 0.29, & 0.20\end{bmatrix}^T \; Nm$. The admittance control gains for all manipulators are designed as $M_{d_i} = 0.5I_6$, $D_{d_i} = 2\sqrt{K_{d_i}}I_6$, $K_{d_i} = 60I_6$. The NTSM control parameters are designed as $\alpha_i = 5/3$, $\beta_i = 1$, $\kappa_i = 10$, and $k_{s_i} = 200$.

The relative positions of the end effectors on the object are $r_1 = \begin{bmatrix}0 & -r & 0\end{bmatrix}^T \; m$, $r_2 = \begin{bmatrix}\sqrt{3}r/2 & r/2 & 0\end{bmatrix}^T \; m$, and $r_3 = \begin{bmatrix}-\sqrt{3}r/2 & r/2 & 0\end{bmatrix}^T \; m$, where $r = 0.05 \; m$. The positions and orientations of the manipulators relative to the world frame are ${}^w\boldsymbol{\delta}^1 = \begin{bmatrix}0 & -2r & 0\end{bmatrix}^T \; m$, ${}^wR^1 = \begin{bmatrix}0 & 0 & 0\end{bmatrix}^T \; m$, ${}^w\boldsymbol{\delta}^2 = \begin{bmatrix}\sqrt{3}r & r & 0\end{bmatrix}^T \; m$, ${}^wR^2 = \begin{bmatrix}0 & 0 & -2\pi/3\end{bmatrix}^T \; m$, ${}^w\boldsymbol{\delta}^3 = \begin{bmatrix}-\sqrt{3}r & r & 0\end{bmatrix}^T \; m$, ${}^wR^3 = \begin{bmatrix}0 & 0 & 2\pi/3\end{bmatrix}^T \; m$. The desired object waypoints are $\boldsymbol{x}_{d1_o} = \begin{bmatrix}0 & 0 & 0.06\end{bmatrix}^T$, $\boldsymbol{x}_{d2_o} = \begin{bmatrix}0.02 & 0 & 0.06\end{bmatrix}^T$, $\boldsymbol{x}_{d3_o} = \begin{bmatrix}-0.02 & -0.02 & 0.06\end{bmatrix}^T$, $\boldsymbol{x}_{d4_o} = \begin{bmatrix}0 & 0.02 & 0.06\end{bmatrix}^T$, and the desired trajectory is generated following a trapezoidal velocity profile. It is assumed that each manipulator is initially positioned so that the object is at the initial desired position. It is assumed that the object remains at an orientation of $\boldsymbol{\xi}_o = \begin{bmatrix}1 & 0 & 0 & 0\end{bmatrix}^T$. Fig. 3 shows the external forces, $\boldsymbol{F}_e$, applied to the object during the simulations.

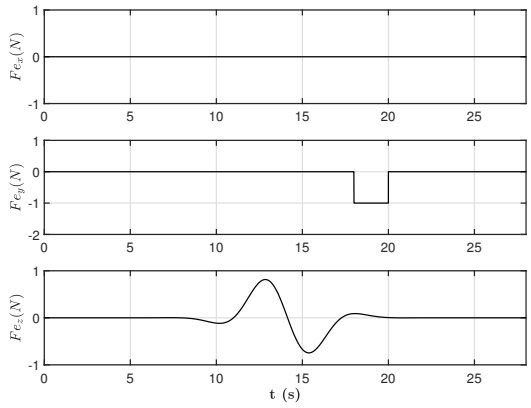

Fig. 3. Applied external forces on the object

B. Simulation Results

The first case considers a centralized scenario with the proposed framework where each manipulator receives the desired trajectory of the object. The manipulator's end-effectors in Cartesian space are shown in each agent's frame in Fig. 4 and in the world frame in Fig. 5. Fig. 4 shows that the reference trajectories accurately track the desired trajectories until the disturbances are applied. Once the disturbances are applied, the admittance controller generates a compliant reference trajectory relative to the applied forces. The actual end-effector position accurately tracks the reference trajectory with the NTSM controller. Note that in Fig. 4 there is a compliant motion in the x-axis of Agents 2 and 3 when a force is applied in the y-axis at around 18 seconds. This occurs because of the relative positions of Agents 2 and 3, which is resolved when the trajectories are transformed to the world frame in Fig. 5. Fig. 5 shows the manipulators accurately tracking the desired trajectory of the object considering the relative grasping positions of the end effectors on the object.

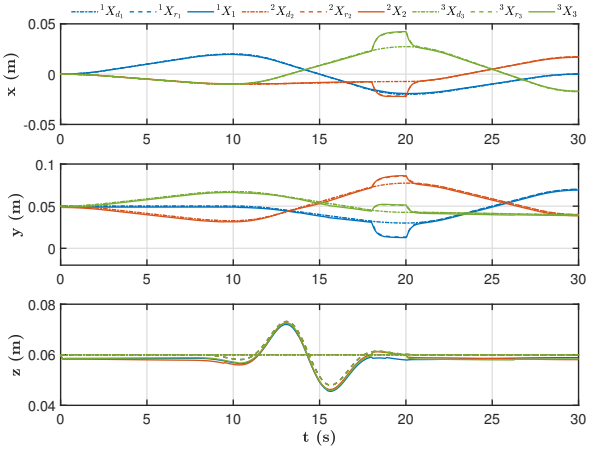

Fig. 4. Centralized admittance-based NTSM control in the agents' frames

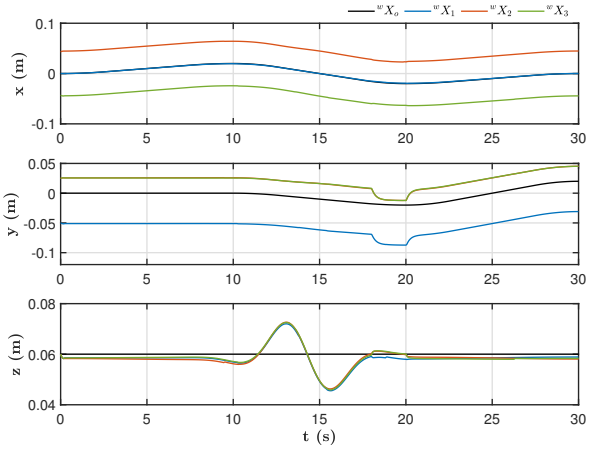

Fig. 5. Centralized admittance-based NTSM control in the world frame

The second case considers a centralized scenario with an impedance controller in place of the admittance-based NTSM controller. The impedance controller is designed as in [15],

$$\boldsymbol{u}_i = -\boldsymbol{h}_{e_i} + \bar{\mathcal{C}}_i(\boldsymbol{q}_i, \dot{\boldsymbol{q}}_i)\dot{\boldsymbol{x}}_i + \bar{\mathcal{G}}_i(\boldsymbol{q}_i) + \bar{\mathcal{M}}_i(\boldsymbol{q}_i)\Big(\ddot{\boldsymbol{x}}_{d_i} - M_d^{-1}(D_d(\dot{\boldsymbol{x}}_i - \dot{\boldsymbol{x}}_{d_i}) + K_d(\boldsymbol{x}_i - \boldsymbol{x}_{d_i})) - \boldsymbol{h}_{e_i}\Big) + \boldsymbol{h}_{d_i}.$$

The impedance gains, M_d, D_d, and K_d, are set equal to the admittance gains to generate the same desired response to external wrenches. Fig. 6 shows the manipulators response in the world frame. The tracking is inaccurate due to the internal frictions and model uncertainties. The impedance gains could be tuned to achieve better tracking, but this would result in a less compliant response. Compared to the impedance control, the proposed framework has higher design flexibility and improved performance in the presence of internal friction and model uncertainties.

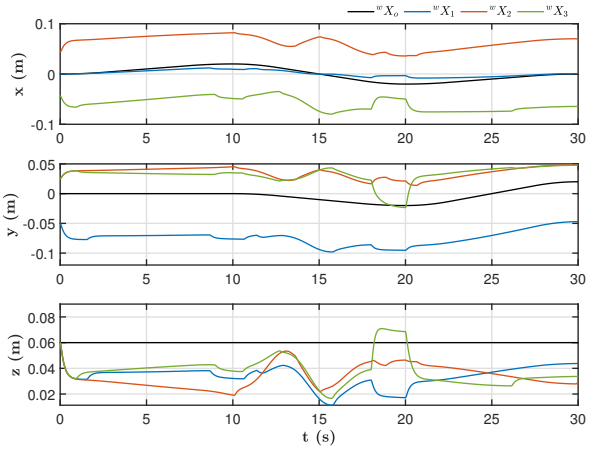

Fig. 6. Centralized impedance control in the world frame

The third case considers a decentralized scenario of the proposed framework with a chain communication structure, where Agent $i+1$ receives information from Agent i. There are time-varying delays in each communication channel of 0.1 ± 0.025 s. In this case, the object is set to be rotated $20°$ about each axis, therefore $\boldsymbol{\xi}_o = \begin{bmatrix}0.96 & 0.14 & 0.20 & 0.14\end{bmatrix}^T$. Fig. 7 shows the accurate tracking of the desired object trajectory and suitable responses to the external forces which are comparable to the centralized case in Fig. 4.

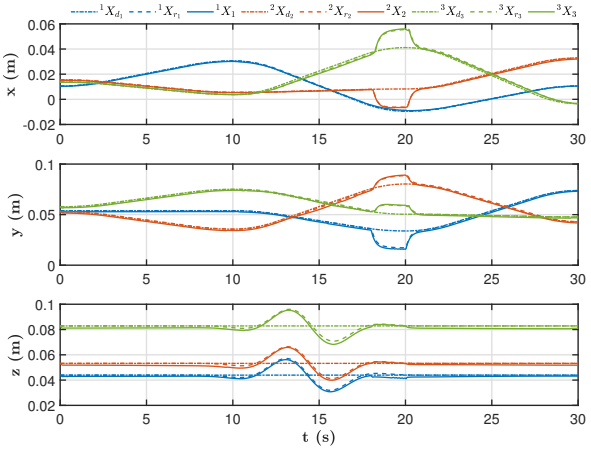

Fig. 7. Decentralized admittance-based NTSM control in the agents' frames

V. Conclusions

The paper proposes a decentralized multi-manipulator framework for cooperative handling of an object. An admittance controller provides a safe, compliant response to physical human interaction. A NTSM controller achieves accurate tracking for manipulators with frictional disturbances and model uncertainties. A distributed method of load allocation is proposed. The framework is validated with numerical simulations of three 3-DOF manipulators, demonstrating significant advantages over classical impedance control. Future work will extend the proposed approach to 7-DOF multi-robotic manipulators with more dexterous manipulations.

References

[1] S. Tarbouriech, B. Navarro, P. Fraisse, A. Crosnier, A. Cherubini, and D. Sallé, "Admittance control for collaborative dual-arm manipulation," in *2019 19th International Conference on Advanced Robotics (ICAR)*. IEEE, 2019, pp. 198–204.

[2] Y. Li, C. Yang, W. Yan, R. Cui, and A. Annamalai, "Admittance-based adaptive cooperative control for multiple manipulators with output constraints," *IEEE transactions on neural networks and learning systems*, vol. 30, no. 12, pp. 3621–3632, 2019.

[3] F. Caccavale, P. Chiacchio, A. Marino, and L. Villani, "Six-dof impedance control of dual-arm cooperative manipulators," *IEEE/ASME Transactions On Mechatronics*, vol. 13, no. 5, pp. 576–586, 2008.

[4] C. Cai, Y.-J. Pan, S. Liu, and L. Wan, "Task space bilateral teleoperation of co-manipulators using power-based tdpc and leader-follower admittance control," in *IECON 2021–47th Annual Conference of the IEEE Industrial Electronics Society*. IEEE, 2021, pp. 1–6.

[5] Y. Feng, X. Yu, and Z. Man, "Non-singular terminal sliding mode control of rigid manipulators," *Automatica*, vol. 38, no. 12, pp. 2159–2167, 2002.

[6] H. Shen, Y.-J. Pan, and L. Wan, "Teleoperated single-master-multiple-slave system for cooperative manipulations in task space," in *2021 4th IEEE International Conference on Industrial Cyber-Physical Systems (ICPS)*. IEEE, 2021, pp. 864–869.

[7] J. Mei, W. Ren, and G. Ma, "Distributed coordinated tracking with a dynamic leader for multiple euler-lagrange systems," *IEEE Transactions on Automatic Control*, vol. 56, no. 6, pp. 1415–1421, 2011.

[8] Z. Ma, Z. Liu, P. Huang, and Z. Kuang, "Adaptive fractional-order sliding mode control for admittance-based telerobotic system with optimized order and force estimation," *IEEE Transactions on Industrial Electronics*, vol. 69, no. 5, pp. 5165–5174, 2021.

[9] R. Kikuuwe, "A sliding-mode-like position controller for admittance control with bounded actuator force," *IEEE/ASME Transactions On Mechatronics*, vol. 19, no. 5, pp. 1489–1500, 2013.

[10] H. Kong, G. Li, and C. Yang, "Non-singular fixed-time sliding mode control for unknown-dynamics manipulators interacting with environment," in *2022 27th International Conference on Automation and Computing (ICAC)*. IEEE, 2022, pp. 1–6.

[11] S. Erhart and S. Hirche, "Internal force analysis and load distribution for cooperative multi-robot manipulation," *IEEE Transactions on Robotics*, vol. 31, no. 5, pp. 1238–1243, 2015.

[12] A. Z. Bais, S. Erhart, L. Zaccarian, and S. Hirche, "Dynamic load distribution in cooperative manipulation tasks," in *2015 IEEE/RSJ International Conference on Intelligent Robots and Systems (IROS)*. IEEE, 2015, pp. 2380–2385.

[13] R. Campa, K. Camarillo, and L. Arias, "Kinematic modeling and control of robot manipulators via unit quaternions: Application to a spherical wrist," in *Proceedings of the 45th IEEE Conference on Decision and Control*. IEEE, 2006, pp. 6474–6479.

[14] L. Wan, Y.-J. Pan, and H. Shen, "Improving synchronization performance of multiple euler-lagrange systems using non-singular terminal sliding mode control with fuzzy logic," *IEEE/ASME Transactions on Mechatronics*, vol. 27, no. 4, pp. 2312–2321, 2022.

[15] H. Sadeghian, L. Villani, M. Keshmiri, and B. Siciliano, "Task-space control of robot manipulators with null-space compliance," *IEEE Transactions on Robotics*, vol. 30, no. 2, pp. 493–506, 2013.